



Article

# Adsorption of Patent Blue V from Textile Industry Wastewater Using *Sterculia alata* Fruit Shell Biochar: Evaluation of Efficiency and Mechanisms

Balendu Shekher Giri <sup>1,2,\*</sup> , Mandavi Goswami <sup>1</sup>, Prabhat Kumar <sup>1</sup>, Rahul Yadav <sup>1</sup> , Neha Sharma <sup>3</sup>, Ravi Kumar Sonwani <sup>1</sup>, Sudeep Yadav <sup>4</sup>, Rajendra Prasad Singh <sup>5</sup>, Eldon R. Rene <sup>6</sup>, Preeti Chaturvedi <sup>2</sup> and Ram Sharan Singh <sup>1,\*</sup>

<sup>1</sup> Department of Chemical Engineering and Technology, Indian Institute of Technology (BHU), Varanasi, Uttar Pradesh 221005, India; mandavigs@gmail.com (M.G.); prabhat.kumar.che15@itbhu.ac.in (P.K.); rahul.yadav.che15@itbhu.ac.in (R.Y.); raviks.rs.che16@itbhu.ac.in (R.K.S.)

<sup>2</sup> Aquatic Toxicology Laboratory, Environmental Toxicology Group, Council of Scientific and Industrial Research-Indian Institute of Toxicology Research (CSIR-IITR), Vishvigyan Bhawan, 31, M.G. Marg, Lucknow, Uttar Pradesh 226001, India; preetichaturvedi@iitr.res.in

<sup>3</sup> Amity Institute of Microbial Technology, Amity University, Noida, Uttar Pradesh 201313, India; nehabinbiochemistry@gmail.com

<sup>4</sup> Department of Chemical Engineering, Bundelkhand Institute of Engineering & Technology (BIET), Jhansi, Uttar Pradesh 284128, India; sudeep2406@gmail.com

<sup>5</sup> Department of Municipal Engineering, Southeast University, Nanjing 210096, China; rajupsc@hotmail.com

<sup>6</sup> Department of Water Supply, Sanitation and Environmental Engineering, IHE Delft Institute for Water Education, P.O. Box 3015, 2601DA Delft, The Netherlands; e.raj@un-ihe.org

\* Correspondence: balendushekher23@gmail.com (B.S.G.); rssingh.che@itbhu.ac.in (R.S.S.)

Received: 8 April 2020; Accepted: 8 July 2020; Published: 16 July 2020



**Abstract:** Biochar prepared from *Sterculia alata* fruit shell showed a better performance for dye removal than the biomass from *Sterculia alata* fruit shell. The important process parameters—namely the pH, the amount of biochar, the initial dye concentration and the contact time—were optimized in order to maximize dye removal using biochar of *Sterculia alata* fruit shell as the bio-sorbent. The results from this study showed that the maximum adsorption of dye on the biochar was obtained at a biochar dosage of 40 g/L, at a contact time of 5 h, and an initial dye concentration of 500 mg/L (pH 2.0; temperature  $30 \pm 5$  °C). The increase in the rate adsorption with temperature and the scanning electron microscopic (SEM) images indicated the possibility of multilayer type adsorption which was confirmed by better fit of the Freundlich adsorption isotherm with the experimental data as compared to the Langmuir isotherm. The values  $n$  and  $R^2$  in the Freundlich isotherm were found to be 4.55 and 0.97, respectively. The maximum adsorption capacity was found to be 11.36 mg/g. The value of  $n > 1$  indicated physical nature of the adsorption process. The first and second order kinetics were tested, and it was observed that the adsorption process followed the first-order kinetics ( $R^2 = 0.911$ ).

**Keywords:** Patent Blue V; Langmuir isotherm; Freundlich isotherm; SEM; removal efficiency

## 1. Introduction

Water pollution due to toxic industrial effluent which contains various pollutants, such as dye, acids, etc., have become a global environmental problem. Dyes or dye components are major pollutants in the effluent from industries such as textiles, pulp and paper, leather, etc. [1,2]. Due to various applications, the production of pigments and dyestuffs is increasing continually and annually ~700,000 tonnes of pigments and dyes are produced in the world, wherein India's contribution is

~80,000 tonnes [3–5]. The dyes exhibit poor biodegradability and, therefore, cause long-term ecological damage. The presence of dye in the water bodies and soil pose various problems including toxicity of water bodies and soil, change in the quality of water, toxicity to the microorganisms/biocatalysts present in the water, percolation of dyes in the underground water through soil, entry in the food chain which result in various health effects on human beings and animals [6,7]. Dye is present at various concentrations in several wastewater streams and it can also cause toxic effects on aquatic organisms, microbes and prevent seed germination [8].

Different techniques such as biological treatment, ozone treatment, adsorption, and chemical oxidation have been tested by the researchers to remove dyes from wastewater. Among all these suggested technologies, adsorption is most promising and considered to be a convenient technique for removal of dyes because of its low cost, easy operation and high removal capacity [9,10]. Nano materials, as adsorbents, also provide various advantages such as high surface area, porous structure and thermal stability [11,12]. However, the production cost of the nano-based materials is still high; hence, it prohibits its application for commercial purposes. Activated carbon is another commonly reported adsorbent for dye removal because it has excellent adsorption capacity [8,13,14]. Nowadays, the application of biochar for wastewater treatment is being explored by different researchers [2]. The major advantage of biochar is its low cost of production, because it is generally produced using agro waste and it provides relatively good adsorption capacity [15], durability, and it may be regenerated and used multiple times [16,17]. Biochar is usually produced using pyrolysis of the biomass. The process parameters during pyrolysis affect the physicochemical characteristics of the biochar [8,16]. Chemical modification of biochar using acids, bases or polymers may result in better adsorption efficiency because of increased surface area, modified chemical functionality and presence of high-affinity adsorption sites [16]. From a kinetic modeling perspective, adsorption isotherms [18,19] are used to describe the mechanism of adsorption on the surface of adsorbent, and these isotherms provide values of kinetic parameters that can be used to design full scale adsorption towers. Adsorption kinetics provides information about the rate at which the pollutant is adsorbed [15]. Generally, first-order, second-order reversible or irreversible and pseudo-first, pseudo-second order models are applied to the experimental data [16].

In this study, biochar prepared using *Sterculia alata* fruit shell, an agro waste, was used to remove Patent Blue V dye from wastewater. This dye is mainly present in the effluent of the carpet and textile industry of Varanasi and Bhadohi, Uttar Pradesh, India. This is the first report that shows the application of *Sterculia alata* fruit shell for preparing biochar, and its ability for dye removal was explored.

## 2. Materials and Methods

### 2.1. Materials (Adsorbate and Adsorbent)

*Sterculia alata* fruit shells were used as the raw material for the production of biochar. It was collected from the trees located in Indian Institute of Technology (BHU) campus, Varanasi, India. The Patent Blue V dye used in this study was purchased from a local chemical supplier. The wavelength (630 nm) corresponding to the maximum absorption was determined using scanning mode of an UV-Visible Spectrophotometer (Elico, Hyderabad, India). The dye stock solution of the required concentration was prepared by dissolving a known amount of dye in distilled water.

### 2.2. Preparation of Biochar

In the first step, the biomass was ground to increase the surface area and then pyrolyzed at 500 °C by increasing the temperature at the rate of 10 °C min<sup>-1</sup> to convert into biochar [20]. Nitrogen was purged in a Pyrolyzer for 60 min at the rate of 100 cm<sup>3</sup> min<sup>-1</sup> to maintain the inert atmosphere. The biochar obtained after pyrolysis was washed with distilled water and thereafter dried at 110 °C and finally impregnated with NaOH to improve its adsorption capacity [21]. The NaOH activation method was used to improve the sorption properties of the tested biochar. Thermally treated biochar (3 g)

was mixed with 40 mL of 4 M NaOH and incubated at room temperature for 2 h, under intermittent shaking (15 min interval) conditions. After NaOH impregnation, the excess solution was discarded with vacuum filtering and the chemically treated solid was dried overnight in an oven at 105 °C. The dried sample was heated in a quartz-tube furnace to 800 °C, at a heating rate of 3 °C min<sup>-1</sup> under inert atmospheric conditions (N<sub>2</sub> flow = 2 L min<sup>-1</sup>) for 2 h. After activation, the samples were taken out from the heating element and cooled down to ambient temperature under nitrogen flow. The activated samples were washed using 2 L of deionized (DI) water followed by 0.1 M HCl solution (200 mL) and washed again with DI water until the pH of filtrates was ~7.0. The washed activated carbon samples were dried in an oven at 105 °C and stored in a desiccator for further analysis. Each activated sample was denoted as “N-treatment temperature AC” (e.g., N-300AC for activated carbon from N-300).

### 2.3. Characterization of Biochar and *Sterculia alata* Biomass

The biochar produced from *Sterculia alata* biomass was characterized in order to evaluate its physico-chemical properties. Scanning electron microscopy (SEM) analysis was performed using a JEOL JSM-6400 Scanning Microscope (JEOL, Tokyo, Japan) with low vacuum of 30 Pa, voltage 20 kV and 10–12 mm working distance from the detector. The results were used to compare the changes in the structural and surface characteristics of the biochar samples before and after treatment of Patent Blue dye V. The effect of adsorption on the porosity was clearly visible from the SEM results shown in Figure 1a,b. Dispersive X-ray Spectroscopy (EDX) with SEM analysis provides rapid qualitative or semi-quantitative analysis of the biochar’s elemental composition [7,22,23]. Elemental analysis on the biochar surface was also conducted at different time intervals, simultaneously with the SEM-EDX (Oxford Instruments Link ISIS, and Oxfordshire, UK) and the results are given in Table 1.

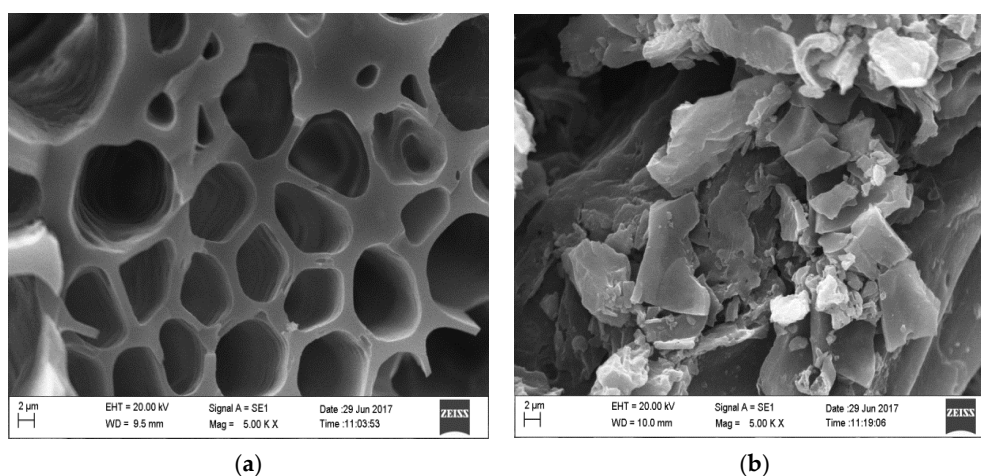


**Figure 1.** SEM morphology of *Sterculia alata* fruit shell biochar for the adsorption of Patent Blue V dye; (a) before adsorption; (b) after adsorption.

**Table 1.** Elemental composition by EDX analysis of biochar and biomass samples.

Elements	Biochar		Biomass	
	Weight %	Atomic %	Weight %	Atomic %
C	72.4	78.7	52.7	61.5
N	6.38	5.95	0	0
O	16.7	13.6	41.6	36.5
P	0.52	0.22	0	0
K	2.76	0.92	5.71	2.05
Mg	0.60	0.32	0	0
Ca	0.68	0.22	0	0

Fourier Transform Infrared (FTIR) analysis of the biochar samples was conducted before and after adsorption of Patent Blue V dye and the results is shown in Table 2. Before FTIR analysis, the biochar samples were well-ground and mixed with KBr solution to 0.1% (wt. basis) and then pressed into pellets to obtain the FTIR spectra. The spectra of these biochar samples were measured using a Bruker Vector 202 FTIR spectrometer (OPUS 2.0 software, Berlin, Germany).

#### 2.4. Batch Adsorption Tests

Batch adsorption tests were conducted in Erlenmeyer flasks ( $V = 250$  mL) and the potential of biochar to remove Patent Blue V dye was ascertained. The flasks contained different initial concentrations of the dye solution (in 100 mL) and known amount of biochar was added according to the desired adsorbent dose. The batch studies were carried out at different temperatures ( $30$  °C,  $35$  °C and  $53$  °C), pH (2.0, 4.0, 6.0, 7.0, 8.0, 9.0, 10.0, 11.0 and 12.0), concentrations of dye in the wastewater (0, 10, 20, 50, 100, 500 mg/L) and adsorbent dose in order to evaluate the optimum process parameters. The final concentration of dye solutions was measured using an UV-visible spectrophotometer at 630 nm, at a fixed contact time. The dye removal (R) was calculated using Equation (1).

$$R = (C_0 - C_t) \times 100/C_0 \quad (1)$$

where,  $C_0$  = initial concentration (mg/L) and  $C_t$  = dye concentration at time,  $t$  (mg/L).

The percentage adsorption of PB (V) dye and equilibrium adsorption capacity,  $q_e$  (mg/g), was calculated using Equations (2) and (3):

$$\text{Adsorption (\%)} = \frac{(C_0 - C_e)}{C_0} \times 100 \quad (2)$$

$$q_e = \frac{(C_0 - C_e)}{W} \times V \quad (3)$$

where  $C_0$  and  $C_e$  are the initial and equilibrium concentrations of PB (V) (mg/L), respectively,  $V$  is the volume of the dye solution (L), and  $W$  is the weight of biochar (g).

#### 2.5. Adsorption Isotherm Models

The Freundlich [24] and Langmuir [7,23] type adsorption models were used to fit the experimental data. The model equations are shown in Equations (4) and (5).

$$\text{Freundlich Isotherm: } \log q = \log K_F + 1/n \times \log C_{eq} \quad (4)$$

$$\text{Langmuir isotherm: } 1/q = 1/q_0 + 1/(K_L - q) \times 1/C_{eq} \quad (5)$$

where  $q$  = amount of dye adsorbed (mg of dye per g of adsorbent);  $K_F$  = parameter related to the adsorption;  $n$  = measure of sorption intensity (value of  $n$  [1, 10]);  $K_L$  = Langmuir constant;  $q_0$  = maximum value of sorption capacity;  $C_{eq}$  = Equilibrium dye concentration (mg/L).

The Langmuir isotherm explains a monolayer adsorption of molecules over a surface having a finite number of adsorption sites of same energy, which are fully available for interaction. The Freundlich isotherm explains about a multilayer adsorption with interaction between the adsorbed molecules over heterogeneous surfaces, assuming that adsorbent surface sites have different binding energies.

**Table 2.** FTIR analysis of biochar and biomass of *Sterculia alata* fruit shell, before and after the adsorption experiments

Biochar before Adsorption		Biomass before Adsorption		Biochar after Adsorption		Biomass after Adsorption	
Wavelength (cm <sup>-1</sup> )	Bond Type	Wavelength (cm <sup>-1</sup> )	Bond Type	Wavelength (cm <sup>-1</sup> )	Bond Type	Wavelength (cm <sup>-1</sup> )	Bond Type
3594.4	O-H (free)	3349.1	Weak N-H (2° amine)	3218.7	O-H (H bonded)	3649.2	O-H (free)
3219.8	O-H (bonded)	2900.6	CH <sub>3</sub> , CH <sub>2</sub> & CH, O-H (very broad)	2930.2	CH <sub>3</sub> , CH <sub>2</sub> , CH (2 or 3 bands)	3299.8	O-H (bending)
2699.3	C-H (aldehydes C-H)	2153.7	Si-H silane,-M=C=O, N=C=S	1971.9	C=C (asymmetric stretch)	3045.2	=C-H & =CH <sub>2</sub>
2258.6	C≡N (sharp)	1728.6	C=O (saturated aldehyde)	1728.3	C=O (saturated aldehydes)	2938.2	CH <sub>3</sub> , CH <sub>2</sub> , CH
1538.6	NH <sub>2</sub> scissoring	1440.3	CH <sub>2</sub> -CH <sub>3</sub> (bending) (1° amine)	1651.3	C=O (amide)	2346.4	Si-H silane, P-H
1435.8	-CH <sub>2</sub> bending	1019.6	P-H bending P-OR esters, Si-OR	1425.5	-CH <sub>2</sub> bending	1565.4	NH <sub>2</sub> scissoring
876.7	=C-H & =CH <sub>2</sub>	889.3	S-OR esters	1043.1	C-O-H bending	1421.1	-CH <sub>2</sub> bending, C-O-H
722.7	C-H bending & ring	714.5	S-OR esters	689.2	C-O, C-N	1195.0	C-N, C-O, C=S,
567.8	C-H deformation	514.3	S-S (disulfide)			1049.3	P-H bending, S=O
						847.3	C-H bending & puckering

## 2.6. Adsorption Kinetics Studies

The kinetic models used in the present study are the pseudo-first and second order models [25]. The pseudo-first order rate equation is described by Equation (6).

$$dq/dt = k_1(q_e - q) \quad (6)$$

where,  $q$  and  $q_e$  are the grams of solute sorbed per gram of sorbent at any time and at equilibrium, respectively, and  $k_1$  is the rate constant.

The pseudo-second order rate equation is described by Equation (7).

$$dq/dt = k_2(q_e - q)^2 \quad (7)$$

where,  $k_2$  is the pseudo-second order rate constant.

## 3. Result and Discussion

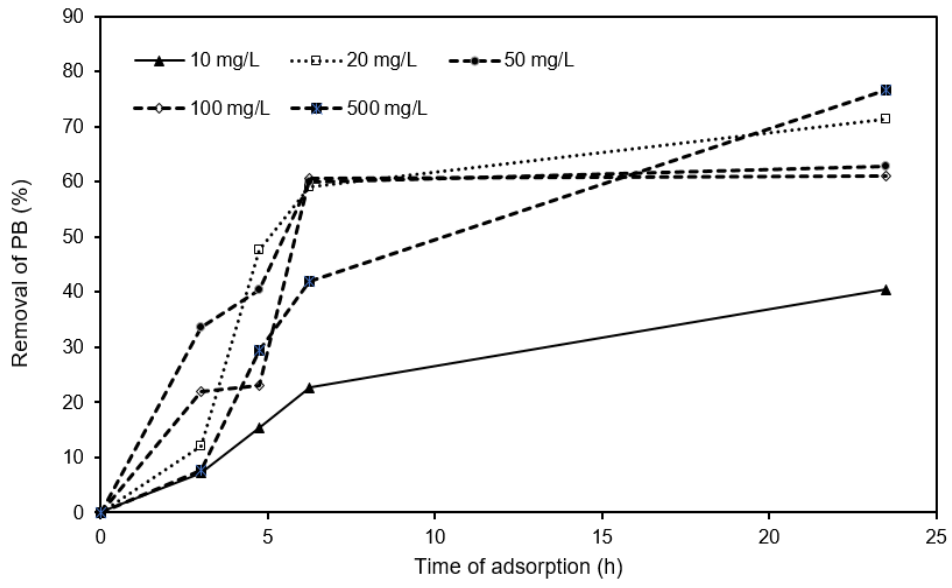
### 3.1. Production of Biochar and Its Characterization

The results from proximate analysis of biochar shows moderately low moisture content (4.18%), high percentage of volatile matter (30.82%), and low ash content (25.94%). High volatile matter lessens the solid yield in the pyrolysis stage while a low inorganic content is important due to the ability to produce a low ash and high fixed carbon content in the biochar. SEM-EDX results show that powdered *Sterculia alata* biochar has 72.4 wt% of carbon and 16.7 wt% of hydrogen and 6.38 wt% oxygen, respectively. It has been reported that, lignin in biomass is highly influential in creating the porous structure of the biochar. The high carbon content (72.4%) was a positive attribute of the prepared biochar. SEM images (Figure 1a) show that the biochar has lot of internal pores with pore size  $>2 \mu\text{m}$ . Usually, higher internal pores provide more active surface area for adsorption, resulting in better adsorption capacity of the material. The SEM image after adsorption (Figure 1b) shows the change in porous structure of biochar after adsorption of the dye molecules. The significant differences observed between the FTIR spectra and functional groups present on the surface of biochar confirm the adsorption of Patent Blue V on the surface of biochar (Table 2).

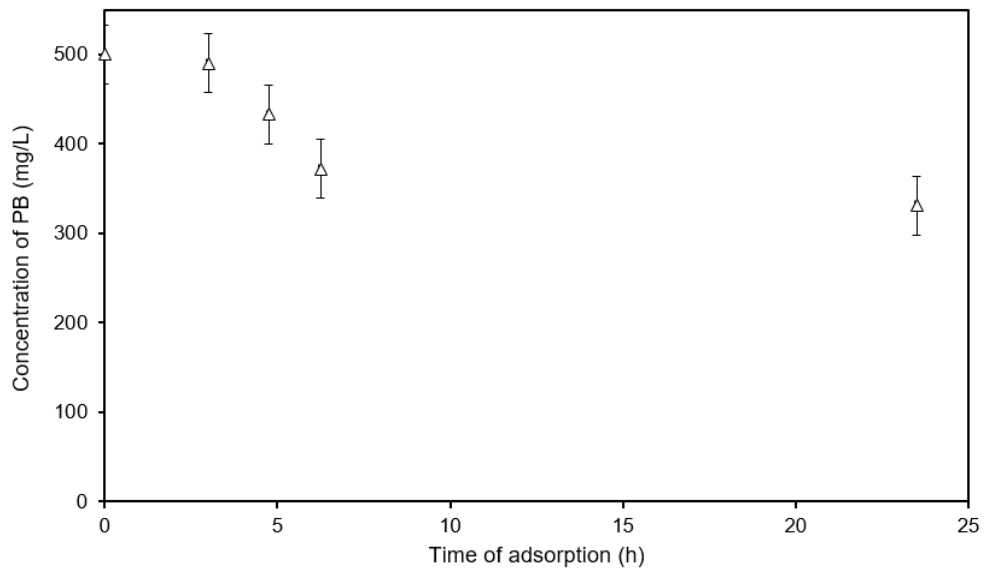
### 3.2. Optimization of the Process Conditions for Maximum Removal of Dye

#### 3.2.1. Effect of pH on the Adsorption of Dye

The effect on Patent Blue V removal was investigated in a pH range varying from 2.0 to 12.0. It was observed that the removal of dye decreased with an increase in pH and the highest PB removal was observed at a pH value of 2.0. As the pH of the solution increases, adsorption of dye was found to decrease due to the reduction in the positive hydrogen ions and increased availability of negatively charged  $\text{OH}^-$  ions, therefore, promoting activities of electrostatic repulsion between the negative charge of the dye and the biochar surface. On the other hand, at an acidic pH; the functional groups of biochar become protonated (Figure 2d). At pH 2.0; the surface of biochar becomes more positively charged, which enhances the adsorption of dye through electrostatic attraction [26–28]. It is clear that the lower pH values ( $<5.0$ ) favor the adsorption process. Therefore, from a commercial application point of view, the operation can be carried out at acidic pH or at the natural pH of the textile wastewater. The maximum adsorption capacity towards PB (V) was found to be 12.34 mg/g at a pH value of 2.0.

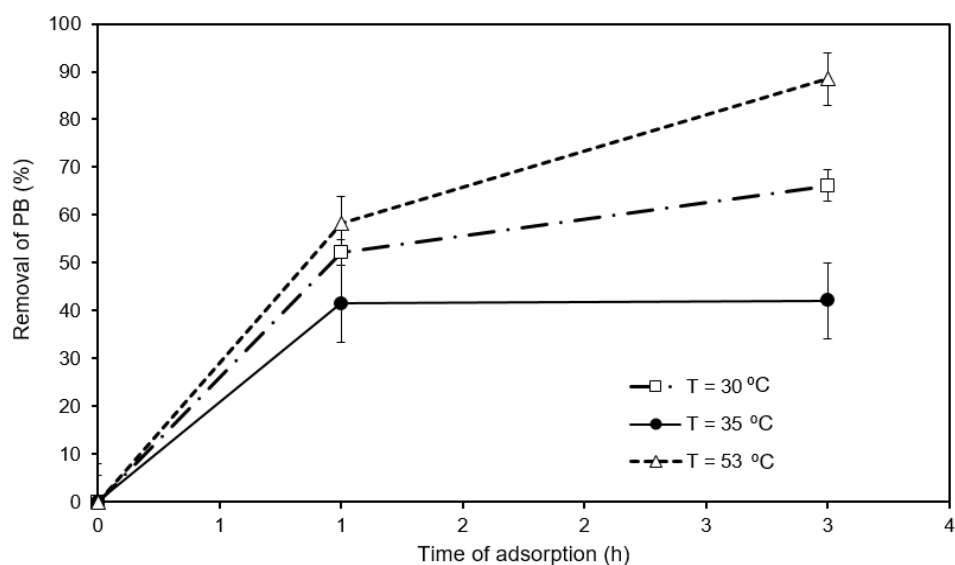


(a)

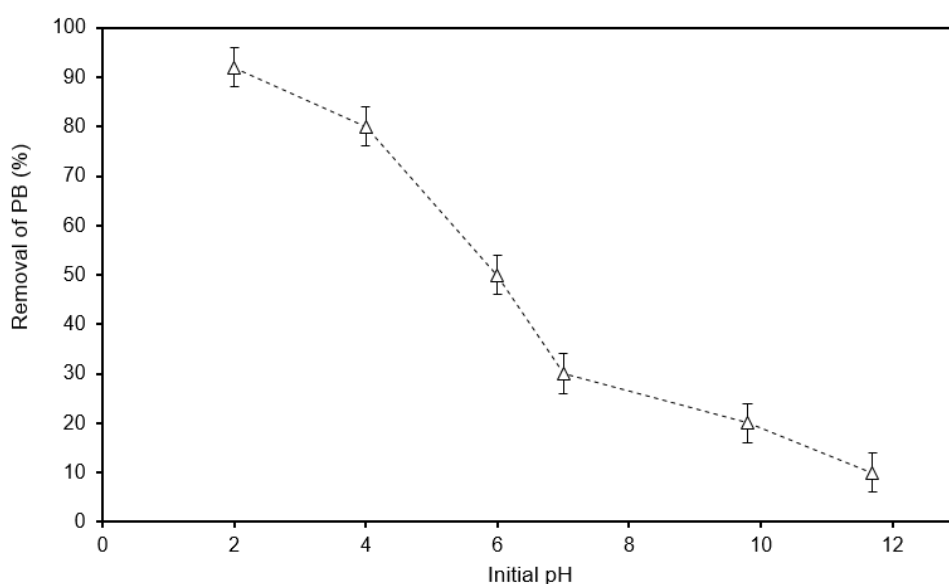


(b)

Figure 2. Cont.



(c)



(d)

**Figure 2.** Effect of process parameters on the removal of PB dye using *Sterculia alata* biochar: (a) removal efficiency profiles; (b) decrease in PB dye concentration with a biochar dose of 4 g; (c) effect of temperature on PB dye removal at an initial concentration of 500 mg/L; (d) effect of pH on the removal efficiency of PB dye.

In another study, the adsorption of PB (V) on ginger waste material was tested and a maximum adsorption capacity of 9.56 mg/g at pH 2.0 and an initial dye concentration of 10 mg/L was reported [29]. Table 3 shows the adsorption capacity of different materials used as adsorbent for the removal of different dyes.

### 3.2.2. Effect of Adsorbent Dosage

A pH value of 2.0 was selected as the optimum pH value for PB adsorption with *Sterculia alata* biochar. The results clearly indicate that 4 g/100 mL or 40 g/L was the optimum dose of the adsorbent for Patent Blue V removal. Similar results were obtained by [20,30–32]. Roy et al. [17] studied the



adsorption of PB by the modified bael shell biochar (BSB) in the pH range of 2.7 to 10.4, and maximum sorption was perceived at pH 2.7. The percentage adsorption values of PB at seven of the tested initial pH values (i.e., 2.7, 4, 6, 7, 8, 9.2 and 10.4) were 74%, 62%, 58%, 55%, 47%, 40% and 39%, respectively. At lower pH values (i.e., 2.7), the surface charge density of BSB was found to be predominantly positive; thus, adsorbing high quantities of anionic PB dye molecules. The maximum adsorption capacity of BSB towards PB (V) was found to be 3.7 mg/g at a pH value of 2.7 (Figure 2d).

**Table 3.** Comparison of the adsorption capacities for different dyes using various types of biochar.

Biochar	Adsorption Capacity (mg/g)	Type of Dye	References
Activated carbon derived from finger citron residue (FAC)	934.58	Methylene Orange	[4]
Activated carbon derived from finger citron residue (FAC)	581.40	Methylene Blue	[4]
Sawdust of the rubber wood ( <i>Hevea brasiliensis</i> )	333.33	Methylene Blue	[33]
Cellulose-based and NaOH—functionalized biochar	234.57	Methylene Blue	[34]
Glucose-based H <sub>2</sub> SO <sub>4</sub> —functionalized biochar	306.13	Methyl Orange	[34]
Ginger waste material (GWM)	9.560	Patent Blue V	[29]
<i>Sterculia alata</i>	11.36	Patent Blue V	This study

### 3.2.3. Effect of Initial Dye Concentration

The results shown in Figure 2a confirm that >50% PB dye removal was achieved within 10 h in the dye solutions at concentrations <50 mg/L. No further removal was observed in these solutions. However, when the PB concentration was 500 mg/L, the removal continuously increased up to 60% after 22 h (Figure 2b). A similar trend has been reported by several researchers [20,30–32]. Considering the good results achieved at 500 mg/L, further experiments were conducted at this initial PB dye concentration.

However, for practical purposes, in order to test higher dye concentrations, i.e., >500 mg/L, future experiments should be performed using fixed bed adsorption columns, either as a stand-alone technology or combine different series of adsorption columns or even consider a combination of advanced oxidation and adsorption based technologies. In such studies, the effect of initial dye concentration, liquid (wastewater) flow rate, pH, bed height and the type of biochar based adsorbent (e.g., rice husk, sugarcane bagasse, saw dust, *Sterculia alata*) added to the fixed bed adsorption column can be tested. Besides, the breakthrough profiles should also be fitted to well-known models such as the Thomas, Yoon-Nelson and Bed Depth Service Time (BDST) models in order to determine the kinetic parameters of the adsorption column.

### 3.2.4. Effect of Contact Time and Temperature

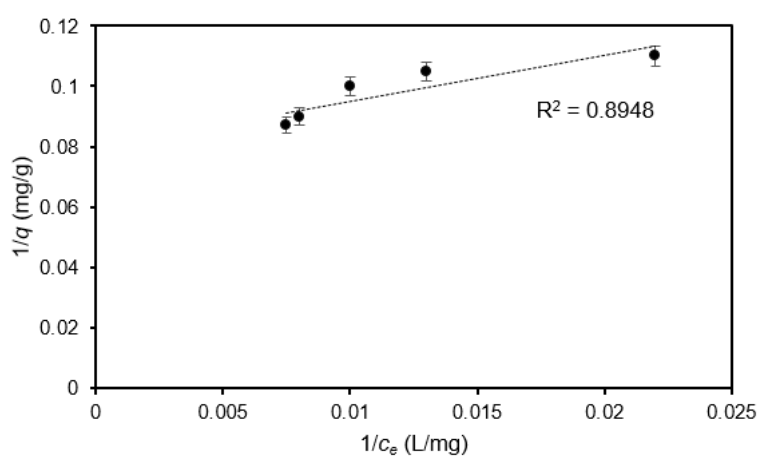
Initially, the rate of adsorption is fast due to the availability of a greater number of active sites on the adsorbent; however, with an increase in the adsorption time, the rate of adsorption decreases and ultimately becomes zero at equilibrium [20,31]. Concerning the effect of temperature, i.e., 30, 35, and 53 °C, increasing the temperature enhanced the removal efficiency of PB dye (Figure 2c). There are several reasons for the increase in adsorption at higher temperatures: (i) the process may be endothermic in nature, which favours more adsorption of the dye molecules at higher temperatures, and (ii) at higher temperatures, due to the intrinsic kinetic energy of the molecules, the dye may be able to penetrate and get adsorbed inside the pores of the adsorbent, resulting in higher rates of adsorption. On the other hand, at higher temperatures, the dye might also undergo thermal degradation and this process could also contribute to the overall removal of dye from wastewater [35].

### 3.2.5. Development of the Adsorption Isotherm

The effect of temperature on the adsorption of PB dye (Figure 2c) in the present study confirms that the rate adsorption increases with temperature, indicating the possibility of multilayer adsorption. The SEM image (Figure 1b) also confirms the multi-layer nature of the adsorption. In order to confirm the nature of adsorption process, Langmuir and Freundlich isotherm models were fitted with the experimental data and the results are given in Table 4, Figure 3a,b, respectively. The results show poor fitting of the data to the Langmuir isotherm, whereas the Freundlich adsorption isotherm satisfactorily fitted the data with an  $R^2$  value of 0.97, thereby confirming the multilayer nature of the adsorption [36]. The value of  $n$  (i.e., the measure of sorption intensity) was found to be more than 4.0 which strongly support the nature of physical adsorption. The adsorption capacity of the biochar was found to be 11.36 mg/g which is better than results reported by other researchers (Table 2) for Patent Blue V dye. Ahmad et al. [37] has reported the adsorption isotherm for Methylene Blue (MB) dye using cow dung biochar, rice husk biochar and sludge biochar. After model fitting, the authors reported that the adsorption behaviour of MB was better explained by the Langmuir model ( $R^2 = 0.996, 0.998$  and  $0.998$ ) when compared to the Freundlich isotherm model ( $R^2 = 0.972, 0.952$  and  $0.715$ ). In another study, Khan et al. [38] reported the MB removal using cow dung biochar, rice husk biochar and sludge biochar and ascertained the  $\log q_e$  values for the two models as 17.50, 17.97, 19.21 mg/g and 1.243, 1.254, and 1.283 mg/g, respectively. Goswami et al. [39] studied the adsorption of Congo red dye using Arjuna seed biochar and reported >90.0% removal in a hybrid treatment system containing biochar, microorganisms and ozone treatment. In another study, Gong et al. [4] reported maximum equilibrium absorption capacities of 934.58 and 581.40 mg/g for Methyl Orange and MB dye, respectively. Mittal and Mishra [40] reported nearly similar values of MB in Gumghatti and  $\text{Fe}_3\text{O}_4$  nanocomposite as ~654 mg/g.

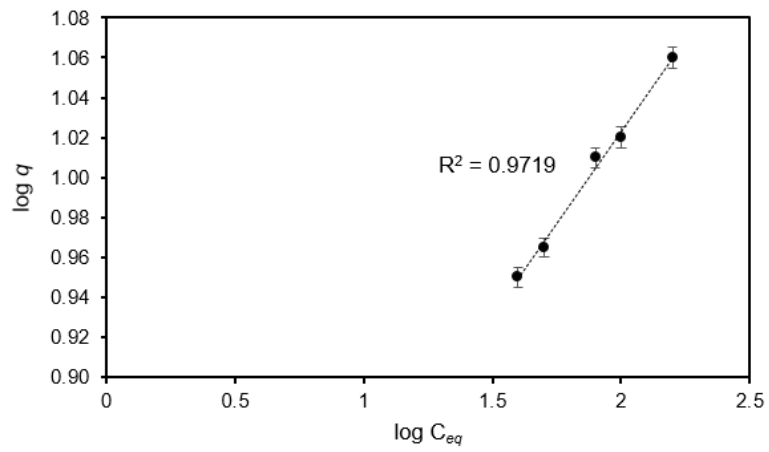
**Table 4.** Model terms and constants for: Freundlich and Langmuir isotherms, first and second order kinetic equations.

Model/Kinetics	Parameters and Units	Values
Freundlich isotherm	$K_f$ (mg/g)	0.97
	$N$	4.55
	$R^2$	0.894
Langmuir isotherm	$K_l$ (mg/g)	0.0706
	$K_f$ (mg/g)	0.336
First order kinetics	$R^2$	0.911
	$K_s$ (mg/g)	0.002
Second order kinetics	$R^2$	0.884

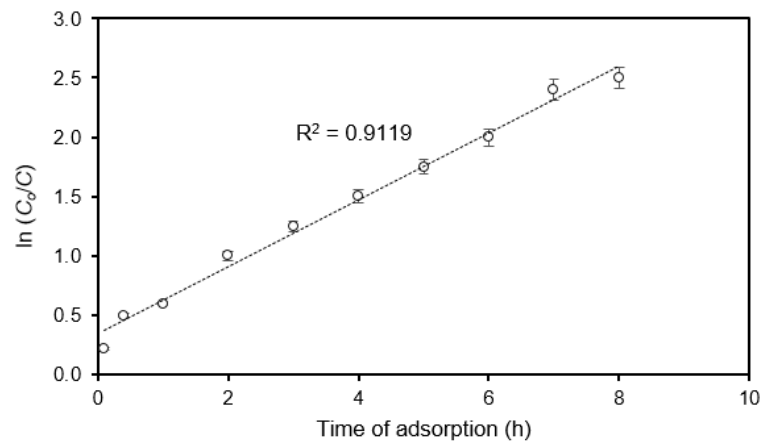


(a)

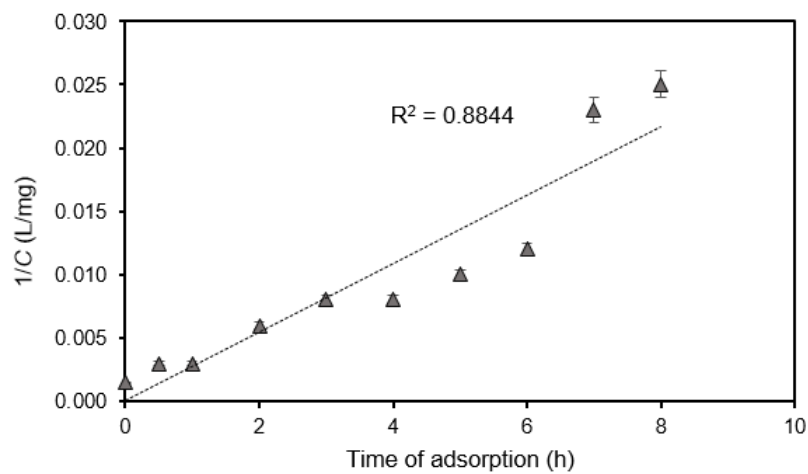
**Figure 3.** Cont.



(b)



(c)



(d)

**Figure 3.** Adsorption of PB dye using *Sterculia alata* biochar: (a) Langmuir isotherm; (b) Freundlich isotherm; (c) pseudo-first order kinetics; (d) pseudo-second order kinetics.

### 3.2.6. Identification of a Suitable Kinetic Model

The pseudo first-order and second-order kinetic equations were fitted with the experimental data (Figure 3c,d and Table 3). The results indicate a good correlation coefficient with the first-order reaction kinetics ( $K_f$ : 0.336 mg/g;  $R^2$ : 0.911) as compared to the second-order reaction kinetics ( $K_f$ : 0.002;  $R^2$ : 0.884). This shows that the adsorption of Patent Blue V dye on biochar depended on the number of adsorption sites [41,42]. In a recent study, Ahmad et al. [37] studied the adsorption of Methylene Blue dye on cow dung biochar, rice husk biochar, and sludge biochar and the kinetics followed the pseudo-second order kinetic model, indicating a chemisorption dominated adsorption process.

### 3.2.7. Effect of Point of Zero Charge

In this study, a 0.1 M NaCl solution was prepared and its initial pH was adjusted from pH 2.0–12.0 using 1 M NaOH and 1 M H<sub>2</sub>SO<sub>4</sub>. Thereafter, 50 mL of 0.1 M NaCl sample was added to 250 mL conical flask and 0.1 g of *Sterculia alata* biochar was added to each solution. The flasks were kept for 24 h and the pH was measured using a pH meter and the values of point of zero charge (pHz) were obtained. It is noteworthy to mention that the functional groups present in *Sterculia alata* biochar had a significant influence on the pHz values. The  $\Delta$ pHz for *Sterculia alata* biochar was found to be 8.0, and this value is close to the value reported by Roy et al. [17] for Bael shell biochar (8.8). In that study, the authors reported that the cationic contaminants can be adsorbed on Bael shell biochar when the pH value is greater than the pHz, while anionic compounds can be adsorbed at pH < pHz. The specific adsorption of cations would shift the value of pHz lower; whereas, in the case of the anions, the value of pHz would shift higher.

### 3.3. Proposed Mechanism for the Adsorption of PB Dye on the *Sterculia alata* Fruit Shell Surface

The adsorption of PB dye over the surface of *Sterculia alata* fruit shell can be explained by hydrogen bonding, electrostatic interactions and van der Waal forces. These interactions can play a vital role in the adsorption process which can be explained as follows: (a) the carboxylic group present on the surface of the *Sterculia alata* fruit shell is expected to completely dissociate at a higher pH (basic medium) which would create an electrostatic repulsion between the carboxylate ion of *Sterculia alata* fruit shell and the anionic part of PB dye resulting in less removal of PB dye from aqueous solution compared to that at the lower pH, (b) the formation of H-bonding between the nitrogen and oxygen containing functional groups of *Sterculia alata* fruit shell and PB dye also affects the PB dye removal process, (c) the van der Waal forces of attraction can come into play due to the presence of hydrophobic parts of *Sterculia alata* fruit shell and PB dye, and (d) the carboxylic and hydroxyl groups are protonated at lower pH (acidic medium), i.e., a pKa value in the range of 3.0 and 5.0 [29] and such a behavior also contributes to better adsorption of the dye molecules. Thus, at the lower value of pH than that of pKa, the carboxylic groups are positively charged, which provides a platform for electrostatic attraction with the SO<sub>3</sub><sup>−</sup> group of PB dye. Anew, the *Sterculia alata* fruit shell provides a positively charged surface for electrostatic interaction with the SO<sub>3</sub><sup>−</sup> group of PB dye at pH < pHz. The functional groups present in *Sterculia alata* fruit shell have a significant influence on the point of zero charge (pHz). Here, it is noteworthy to mention that cationic contaminants can be adsorbed on *Sterculia alata* fruit shell when pH > pHz, while anionic compounds can be adsorbed at pH < pHz. The specific adsorption of cations would shift the value of pHz lower, whereas for that of anions, the value of pHz would shift higher.

The explanation for the interaction of PB dye on the surface of *Sterculia alata* fruit shell is supported by major differences in the FTIR analysis of *Sterculia alata* fruit shell before and after adsorption at a pH value of ~2.34. One observation has been confirmed through the results of FTIR data. The peak at 3408.7 cm<sup>−1</sup> (Table 2) which represents the presence of H bonded -O-H- stretching vibrations of hydroxyl groups from organic acids, alcohols and phenols in *Sterculia alata* fruit shell. It also diminishes after adsorption with PB dye which confirms the hydrogen bond formation between the amine groups of PB dye and hydroxyl group of *Sterculia alata* fruit shell. The protonation of hydroxyl groups and carboxylic

groups occurs at lower pH (2.34) which results in the electrostatic interaction between the anionic PB dye and protonated groups. Furthermore, the shift in the peak value of *Sterculia alata* fruit shell from  $2523.7\text{ cm}^{-1}$  to  $2463.9\text{ cm}^{-1}$  after adsorption signifies the interaction of -O-H- bond of carboxylic acid group with the dye molecules. The appearance of new peak at  $2889.5\text{ cm}^{-1}$  indicates the -CH stretching, and broadened and strengthened peaks were observed at  $1308.1\text{ cm}^{-1}$  for the *Sterculia alata* fruit shell after adsorption compared to that of the peak before adsorption at  $1309.8\text{ cm}^{-1}$ , corresponding to the -SO<sub>3</sub> group. Based on above discussion, a mechanism was proposed for the adsorption of PB dye using *Sterculia alata* fruit shell (Figure 4). Indeed, from a practical perspective, pre-treatment of the biomass (i.e., the *Sterculia alata* fruit shell biochar) will result in additional operating costs that include the costs to operate physical and chemical unit processes. Besides, the reactors' behavior should be optimized statistically and tests should be performed under steady and transient conditions to understand the stability of the process during long term operations [41,42]. The operational costs, i.e., in terms of energy consumption, should also be considered when the adsorption process is scaled up from the lab to pilot and industrial scales.

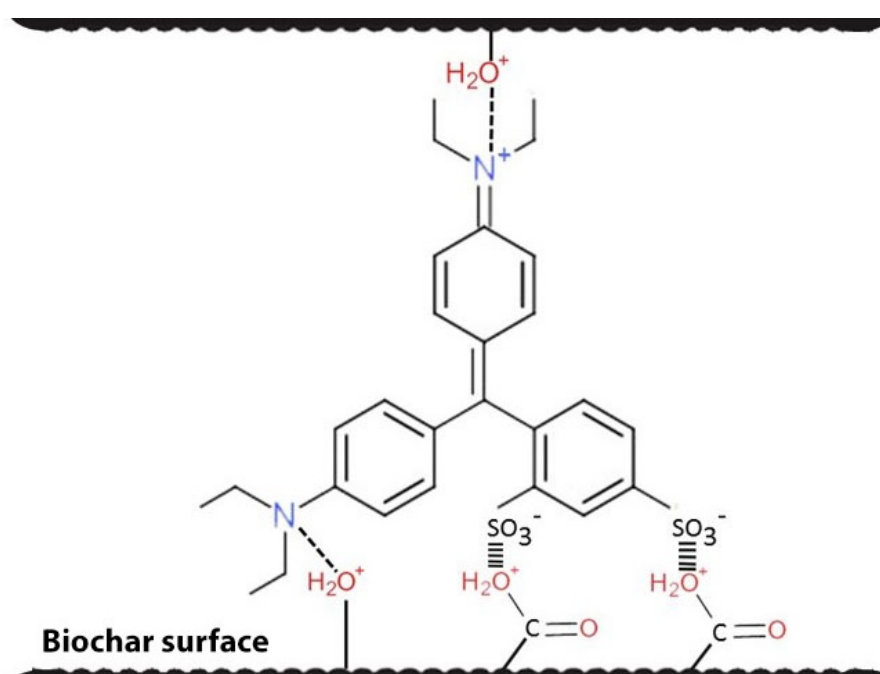


**Figure 4.** Proposed mechanism of Patent Blue V dye adsorption onto *Sterculia alata* fruit shell biochar (adapted from Roy et al. [17]).

#### 4. Conclusions

The *Sterculia alata* fruit shell is an agro waste and it was converted into biochar by pyrolysis. The results obtained from this study are quite promising because the modified biochar was able to remove >80%, at an initial PB dye concentration of 500 mg/L. The high removal capacity of the biochar indicated the possibility of multilayer adsorption and this mechanism was supported by SEM results, and the results from Freundlich isotherm fit. The value of  $n$  (i.e., the measure of sorption intensity) was found to be >4.0 which strongly supports the nature of physical adsorption. The adsorption capacity of the biochar for PB dye was found to be 11.4 mg/g.

**Author Contributions:** Conceptualization, B.S.G., R.P.S., E.R.R. and R.S.S.; Methodology, B.S.G. and R.S.S.; Software, M.G., N.S. and R.K.S.; Validation, P.K., R.Y., M.G., N.S. and R.K.S.; Formal Analysis, P.K., R.Y., M.G., N.S. and R.K.S.; Writing—Original Draft Preparation, B.S.G., P.K., S.Y., R.Y., M.G., N.S. and R.K.S.; Writing—Review and Editing, R.P.S., E.R.R. and R.S.S.; Supervision, P.C., E.R.R. and R.S.S. All authors have read and agreed to the published version of the manuscript.

**Funding:** This research received funding from Design and Innovation Hub (DIH)—Project Varanasi.

**Acknowledgments:** The authors are thankful to Sudheer Kumar for the preparation of biochar at the Department of Chemical Engineering and Technology, IIT (BHU), Varanasi. The authors also acknowledge the Design and Innovation Hub (DIH)—Project Varanasi for providing financial support. The authors thank the staffs from SAIF department providing some analytical support. ERR thanks IHE Delft, The Netherlands for providing staff time support (Support to Society) to collaborate with researchers from IIT (BHU), Varanasi, India. The authors are highly thankful to Director, CSIR-Indian Institute of Toxicology Research (IITR), Lucknow (India) for his valuable encouragement.

**Conflicts of Interest:** The authors declare no conflict of interest. The funding sponsors had no role in the design of the study; in the collection, analyses, or interpretation of data; in the writing of the manuscript, and in the decision to publish the results.

## References

1. El-Qada, E.N.; Allen, S.; Walker, G. Adsorption of basic dyes from aqueous solution onto activated carbons. *Chem. Eng. J.* **2008**, *135*, 174–184. [[CrossRef](#)]
2. Vikrant, K.; Giri, B.S.; Raza, N.; Roy, K.; Kim, K.H.; Rai, B.N.; Singh, R.S. Recent advancements in bioremediation of dye: Current status and challenges. *Bioresour. Technol.* **2018**, *253*, 355–367. [[CrossRef](#)] [[PubMed](#)]
3. Mathur, N.; Bhatnagar, P.; Bakre, P. Assessing mutagenicity of textile dyes from Pali (Rajasthan) using AMES bioassay. *Appl. Ecol. Env. Res.* **2005**, *4*, 111–118. [[CrossRef](#)]
4. Gong, R.; Ye, J.; Dai, W.; Yan, X.; Hu, J.; Hu, X.; Li, S.; Huang, H. Adsorptive removal of methyl orange and methylene blue from aqueous solution with finger-citron-residue-based activated carbon. *Ind. Eng. Chem. Res.* **2013**, *52*, 14297–14303. [[CrossRef](#)]
5. Nidheesh, P.V.; Zhou, M.; Oturan, M.A. An overview on the removal of synthetic dyes from water by electrochemical advanced oxidation processes. *Chemosphere* **2018**, *197*, 210–227. [[CrossRef](#)]
6. Kureel, M.K.; Geed, S.R.; Giri, B.S.; Shukla, A.K.; Rai, B.N.; Singh, R.S.M. Removal of aqueous benzene in the immobilized batch and continuous packed bed bioreactor by isolated *Bacillus sp.* M1. *Resour. Effic. Technol.* **2016**, *2*, S87–S95. [[CrossRef](#)]
7. Kanjanarong, J.; Giri, B.S.; Jaisi, D.P.; Oliveira, F.R.; Boonsawang, P.; Chaiprapat, S.; Singh, R.S.; Balakrishna, A.; Khanal, S.K. Removal of hydrogen sulfide generated during anaerobic treatment of sulfate-laden wastewater using biochar: Evaluation of efficiency and mechanisms. *Bioresour. Technol.* **2017**, *234*, 115–121. [[CrossRef](#)]
8. Talha, M.A.; Goswami, M.; Giri, B.S.; Sharma, A.; Rai, B.N.; Singh, R.S. Bioremediation of Congo red dye in immobilized batch and continuous packed bed bioreactor by *Brevibacillus parabrevis* using coconut shell bio-char. *Bioresour. Technol.* **2018**, *252*, 37–43. [[CrossRef](#)]
9. Zheng, L.; Wang, C.; Shu, Y.; Yan, X.; Li, L. Utilization of diatomite/chitosan-Fe (III) composite for the removal of anionic azo dyes from wastewater: Equilibrium, kinetics and thermodynamics. *Colloids Surf. A* **2015**, *468*, 129–139. [[CrossRef](#)]
10. Garg, V.K.; Gupta, R.; Yadav, A.B.; Kumar, R. Dye removal from aqueous solution by adsorption on treated sawdust. *Bioresour. Technol.* **2003**, *89*, 121–124. [[CrossRef](#)]
11. Gautam, U.K.; Panchakarla, L.S.; Dierre, B.; Fang, X.; Bando, Y.; Sekiguchi, T.; Govindaraj, A.; Golberg, D.; Rao, C.N.R. Solvothermal synthesis, cathodoluminescence, and field-emission properties of pure and N-doped ZnO nano bullets. *Adv. Funct. Mater.* **2009**, *19*, 131–141. [[CrossRef](#)]
12. Chen, R.; Wang, W.; Zhao, X.; Zhang, Y.; Wu, S.; Li, F. Rapid hydrothermal synthesis of magnetic  $\text{Co}_x\text{Ni}_{1-x}\text{Fe}_2\text{O}_4$  nanoparticles and their application on removal of Congo red. *Chem. Eng. Sci.* **2014**, *242*, 226–233. [[CrossRef](#)]
13. Vikrant, V.; Kim, K.H.; Szulejko, J.E.; Pandey, S.K.; Singh, R.S.; Giri, B.S.; Brown, R.J.C.; Lee, S.H. Bio-filters for the treatment of VOCs and odors-A review. *Asian J. Atmos. Environ. (AJAE)* **2017**, *11*, 139–152. [[CrossRef](#)]
14. Vikrant, K.; Kim, K.H.; Ok, Y.S.; Tsang, D.C.W.; Tsang, Y.F.; Giri, B.S.; Singh, R.S. Engineered/designer biochar for the removal of phosphate in water and wastewater. *Sci. Total Environ.* **2018**, *616*, 1242–1260. [[CrossRef](#)] [[PubMed](#)]
15. Giri, B.S.; Goswami, M.; Singh, R.S. Review on application of agro-waste biomass biochar for adsorption and bioremediation dye. *Biomed. J. Sci. Tech. Res.* **2017**, *1*, 1–3.

16. Bharti, V.; Shahi, A.; Geed, S.R.; Kureel, M.K.; Rai, B.N.; Kumar, S.; Giri, B.S.; Singh, R.S. Biodegradation of reactive orange 16 (RO-16) dye in packed bed bioreactor using seeds of Ashoka and Casuarina as packing medium. *Indian J. Biotechnol.* **2017**, *16*, 216–221.
17. Roy, K.; Verma, K.M.; Vikrant, K.; Goswami, M.; Sonwani, R.K.; Rai, B.N.; Vellingiri, K.; Kim, K.H.; Giri, B.S.; Singh, R.S. Removal of Patent Blue (V) Dye using Indian bael shell biochar: Characterization, application and kinetic studies. *Sustainability* **2018**, *10*, 2669. [[CrossRef](#)]
18. Rai, M.K.; Giri, B.S.; Nath, Y.; Bajaj, H.; Soni, S.; Singh, R.P.; Singh, R.S.; Rai, B.N. Adsorption of hexavalent chromium from aqueous solution by activated carbon prepared from almond shell: Kinetics, equilibrium and thermodynamics study. *J. Water Supply: Res. Technol. (Aqua)* **2018**, *67*, 724–737. [[CrossRef](#)]
19. Kumar, M.; Giri, B.S.; Kim, K.H.; Singh, R.P.; Rene, E.R.; López, M.E.; Rai, B.N.; Singh, H.; Prasad, D.; Singh, R.S. Performance of a biofilter with compost and activated carbon based packing material for gas-phase toluene removal under extremely high loading rates. *Bioresour. Technol.* **2019**, *285*, 121317. [[CrossRef](#)]
20. Chaukura, N.; Murimba, E.C.; Gwenzi, W. Synthesis, characterization and methyl orange adsorption capacity of ferric oxide-biochar-nano-composites derived from pulp and paper sludge. *Appl. Water Sci.* **2017**, *7*, 2175–2186. [[CrossRef](#)]
21. Park, J.; Hung, I.; Gan, Z.; Rojas, O.J.; Lim, K.H.; Park, S. Activated carbon from biochar: Influence of its physicochemical properties on the sorption characteristics of phenanthrene. *Bioresour. Technol.* **2013**, *149*, 383–389. [[CrossRef](#)]
22. Singhania, R.R.; Patel, A.K.; Thomas, L.; Goswami, M.; Giri, B.S.; Pandey, A. Industrial enzymes. In *Industrial Biorefineries & White Biotechnology*; Pandey, A., Höfer, R., Taherzadeh, M., Nampoothiri, M., Larroche, C., Eds.; Elsevier: Amsterdam, The Netherlands, 2015; pp. 473–497.
23. Singh, K.; Giri, B.S.; Sahi, A.; Geed, S.R.; Kureel, M.K.; Singh, S.; Dubey, S.K.; Rai, B.N.; Kumar, S.; Upadhyay, S.N.; et al. Biofiltration of xylene using wood charcoal as the biofilter media under transient and high loading conditions. *Bioresour. Technol.* **2017**, *242*, 351–358. [[CrossRef](#)]
24. Yan, X.M.; Shi, B.Y.; Lu, J.J.; Feng, C.H.; Wang, D.S.; Tang, H.X. Adsorption and desorption of atrazine on carbon nanotubes. *J. Colloid Interface Sci.* **2008**, *321*, 30–38. [[CrossRef](#)]
25. Ncibi, M.C.; Mahjouba, B.; Hamissaa, A.M.B.; Mansour, R.B.; Seffena, B. Studies on the biosorption of textile dyes from aqueous solutions using *Posidonia ceanica*. *J. Hazard. Mater.* **2007**, *139*, 280–285. [[CrossRef](#)]
26. Aysan, H.; Edebali, S.; Karakayaet, N. Use of chabazite, a naturally abundant zeolite, for the investigation of the adsorption kinetics and mechanism of methylene blue dye. *Micropor. Mesopor. Mat.* **2016**, *235*, 78–86. [[CrossRef](#)]
27. Zhang, X.; Cheng, C.; Zhao, J.; Ma, L.; Sun, S.; Zhao, C. Polyethersulfone enwrapped graphene oxide porous particles for water treatment. *Chem. Eng. J.* **2013**, *215–216*, 72–81. [[CrossRef](#)]
28. Rahimi, S.; Moattari, R.M.; Rajabi, L.; Derakhshan, A.A.; Keyhani, M. Iron oxide/hydroxide (a, c-FeOOH) nanoparticles as high potential adsorbents for lead removal from polluted aquatic media. *J. Ind. Eng. Chem.* **2015**, *23*, 33–43. [[CrossRef](#)]
29. Ahmad, R.; Kumar, R. Adsorption study of patent blue VF using ginger waste material. *J. Iran. Chem. Res.* **2008**, *1*, 85–94.
30. Desta, M.B. Batch sorption experiments: Langmuir and Freundlich isotherm studies for the adsorption of textile metal ions onto teff straw (*Eragrostis tef*) agricultural waste. *J. Thermodyn.* **2013**, *2013*, 375830. [[CrossRef](#)]
31. Khan, M.M.R.; Mukhlis, M.Z.B.; Mazumder, M.S.I.; Ferdous, K.; Prasad, D.M.R.; Hassan, Z. Uptake of Indosol Dark-blue GL dye from aqueous solution by water hyacinth roots powder: Adsorption and desorption study. *Int. J. Environ. Sci. Technol.* **2014**, *11*, 1027–1034. [[CrossRef](#)]
32. Ghani, W.A.W.A.K.; Mohd, A.; Mahmoud, D.K.; Rebitanim, N.Z.; Sanyang, L.; Zainudin, R.B. Adsorption of methylene blue on sawdust-derived biochar and its adsorption isotherms. *J. Purity Utility React. Environ.* **2013**, *2*, 34–50.
33. Caglar, E.; Donar, Y.O.; Sinag, A.; Birogul, I.; Bilge, S.; Aydinca, K.; Pliekhov, O. Adsorption of anionic and cationic dyes on biochars, produced by hydrothermal carbonization of waste biomass: Effect of surface functionalization and ionic strength. *Turk. J. Chem.* **2018**, *42*, 86–99. [[CrossRef](#)]
34. Al-Degs, Y.S.; El-Barghouthi, M.I.; El-Sheikh, A.H.; Walker, G.M. Effect of solution pH, ionic strength, and temperature on adsorption behavior of reactive dyes on activated carbon. *Dyes. Pigm.* **2008**, *77*, 16–23. [[CrossRef](#)]

35. Lee, C.R.; Kim, H.S.; Jang, I.H.; Im, J.H.; Park, N.J. Pseudo first-order adsorption kinetics of N719 dye on TiO<sub>2</sub> surface. *ACS Appl. Mater. Interfaces* **2011**, *3*, 1953–1957. [[CrossRef](#)] [[PubMed](#)]
36. Ahmad, A.; Khan, N.; Giri, B.S.; Chowdhary, P.; Chaturvedi, P. Removal of methylene blue dye using rice husk, cow dung and sludge biochar: Characterization, application, and kinetic studies. *Bioresour. Technol.* **2020**, *306*, 123202. [[CrossRef](#)] [[PubMed](#)]
37. Khan, N.; Chowdhary, P.; Ahmad, A.; Giri, B.S.; Chaturvedi, P. Hydrothermal liquefaction of rice husk and cow dung in mixed-bed-rotating pyrolyzer and application of biochar for dye removal. *Bioresour. Technol.* **2020**, *309*, 123294. [[CrossRef](#)]
38. Goswami, M.; Chaturvedi, P.; Sonwani, R.K.; Gupta, A.D.; Singhanian, R.R.; Giri, B.S.; Rai, B.N.; Singh, H.; Yadav, S.; Singh, R.S. Application of Arjuna (*Terminalia arjuna*) seed biochar in hybrid treatment system for the bioremediation of Congo red dye. *Bioresour. Technol.* **2020**, *307*, 123203. [[CrossRef](#)]
39. Mittal, H.; Mishra, S.B. Gum ghatti and Fe<sub>3</sub>O<sub>4</sub> magnetic nanoparticles based nanocomposites for the effective adsorption of rhodamine B. *Carbohydr. Polym.* **2014**, *101*, 1255–1264. [[CrossRef](#)]
40. El-Said, A.G.; Badawy, N.A.; Abdel-Aal, A.Y.; Garamon, S.E. Optimization parameters for adsorption and desorption of Zn(II) and Se(IV) using rice husk ash: Kinetics and equilibrium. *Ionics* **2011**, *17*, 263–270. [[CrossRef](#)]
41. Ruziwa, D.; Chaukura, N.; Gwenzi, W.; Pumure, I. Removal of Zn<sup>2+</sup> and Pb<sup>2+</sup> ions from aqueous solution using sulphonated waste polystyrene. *J. Environ. Chem. Eng.* **2015**, *3*, 2528–2537. [[CrossRef](#)]
42. Yu, B.; Xu, J.; Liu, J.H.; Yang, S.T.; Luo, J.; Zhou, Q.; Wan, J.; Liao, R.; Wang, H.; Liu, Y. Adsorption behavior of copper ions on graphene oxide-chitosan aero gel. *J. Environ. Chem. Eng.* **2013**, *1*, 1044–1050. [[CrossRef](#)]



© 2020 by the authors. Licensee MDPI, Basel, Switzerland. This article is an open access article distributed under the terms and conditions of the Creative Commons Attribution (CC BY) license (<http://creativecommons.org/licenses/by/4.0/>).